

Cox Point Processes for Multi Altitude LEO Satellite Networks

Chang-Sik Choi, *Member, IEEE*, and François Baccelli

Abstract—To model existing or future Low Earth Orbit (LEO) satellite networks with multiple constellations, we propose a simple analytical approach to represent the clustering of LEO satellites on orbits, based on a Cox point process. More precisely, we develop a variable-altitude Poisson orbit process that effectively captures the geometric fact that satellites are always positioned on orbits, and these orbits may vary in altitude. Conditioned on the orbit process, satellites situated on these orbits are modeled as Poisson point processes, thereby forming a Cox point process. For this model, we derive useful statistics, including the distribution of the distance to the nearest visible satellite, the outage probability, the Laplace functional of the proposed Cox satellite point process, and the Laplace transform of the interference from the Cox-distributed satellites under general fading. The derived statistics enable the evaluation of the performance of LEO satellite communication systems as functions of network parameters.

Index Terms—LEO satellite communications, stochastic geometry, Cox point process, various altitude LEO satellites, multiple LEO satellite constellations

I. INTRODUCTION

A. Motivation and Background

LEO satellites provide global connectivity to millions of devices on Earth [1]–[5]. The applications of LEO satellite networks are numerous [1]: they provide Internet connections to devices where ground infrastructure is unavailable [2]; localization and emergency communications of aerial and ground devices can be enabled by LEO satellites [3]; LEO satellite networks provide cheaper Internet connections to developing countries [4]. LEO satellite networks can even be integrated with terrestrial networks to enable reliable connections to devices in a small area [5]. To support these applications, LEO satellite networks will have a very large number of satellites.

The viability and performance of LEO satellite communications are significantly determined by the way satellites are distributed in space. Various evaluation methodologies have been proposed to obtain the performance of LEO satellite communication networks. For satellite layout, some studies used probabilistic approaches including a binomial point process [6]–[9]. In contrast to the simulation-based approach, the benefits of employing such analytical models lie in the fact that they presents large-scale behaviors as functions of network key parameters such as the mean number of satellites, their altitudes, etc. Nevertheless, the binomial satellite point

processes in [6]–[9] were not able to incorporate the fact that the satellites are located on approximately circular trajectories around the Earth, namely their orbits. In this paper, we provide a tractable model that incorporates this fact in the multi-altitude LEO satellite case, by generalizing the work in [10] where all orbits are at the same altitude. Specifically, we present an analytical framework leveraging a Cox point process so that orbits are created first according to a Poisson point process on a cuboid and then satellites are distributed as Poisson point processes conditionally on these orbits. We derive key statistical properties of the proposed network model that are critical to obtain the performance of such satellite networks as functions of the altitude distribution, of the mean number of orbits, of the number of satellites, and of the Laplace transform of the random variable representing fading.

B. Contributions

Modeling of variable orbit LEO satellite constellations:

This paper accounts for the geometric properties of practical LEO satellite systems that (i) satellites are always on orbits around the Earth and (ii) such orbits are possibly at different altitudes. By developing a nonhomogeneous Poisson point process of mean λ in a cuboid, we creates a Poisson orbit process of orbits in the Euclidean space. Then, conditionally on the orbit process, satellites are distributed as linear Poisson point processes of mean μ on these orbits. Our motivation is to represent a general LEO satellite network where satellites are located at different altitude bands.

Statistical properties of the proposed Cox point process:

The proposed satellite Cox point process is designed to remain invariant under all rotations of the reference space. This ensures that the network’s statistical properties are consistent from all points on Earth. Leveraging this feature, we derive the probability distribution function for the distance between the typical user and its nearest visible satellite and subsequently derive the outage probability of the proposed network model. Using these results, we derive the Laplace functional of the proposed satellite Cox point process and provide an integral expression for the Laplace transform of total interference. These formulas are directly employed to assess network performance metrics, such as the Signal-to-Interference-plus-Noise Ratio (SINR) of the typical user within future LEO satellite networks consisting of multiple constellations, each characterized by distinct geometric parameters. Finally, as an example illustrating the application of the proposed model, we compare the coverage probability of the proposed Cox model with that of a future Starlink 2A constellation and an existing

Chang-Sik Choi is with Dept. of EE, Hongik University, South Korea. François Baccelli is with Inria Paris and Telecom Paris, France. (email: chang-sik.choi@hongik.ac.kr, francois.baccelli@inria.fr)

Last revised: November 16, 2023

binomial-based LEO satellite model. This comparison reveals that the proposed Cox model has the potential to effectively approximate existing or future LEO satellite constellations.

II. COX-MODELED SATELLITES

A. Satellite Distribution

The center of the Earth is $O = (0, 0, 0)$ and it is of radius r_e . The xy -plane is the reference plane and the x -axis is longitude reference direction. In this paper, we only focus on the snapshot of the network geometry and the movement of satellites is out of the scope.

Consider a cuboid $\mathcal{C} = [r_a, r_b] \times [0, \pi] \times [0, \pi]$ where $r_a \leq r_b$ the minimum and maximum altitudes and a Poisson point process Ξ of intensity measure $\lambda \nu(d\rho) \sin(\phi)/2\pi$ in the cuboid \mathcal{C} . We have $\int_{r_a}^{r_b} \nu(d\rho) = 1$. Then, we build an orbit process by mapping each point of Ξ , say (ρ, θ, ϕ) into an orbit $l(\rho, \theta, \phi)$ in the Euclidean space. Specifically, the first coordinate ρ is the orbit's radius, θ is the orbit's longitude, and ϕ is the orbit's inclination. For the Poisson point process on the cuboid, we write $\Xi = \sum_i Z_i$, where Z_i is the point of Ξ . Since there are on average λ points of Ξ , there are on average λ orbits. The orbit process \mathcal{O} in \mathbb{R}^3 is given by

$$\mathcal{O} = \bigcup_{Z_i \in \Xi} l(\rho_i, \theta_i, \phi_i). \quad (1)$$

Conditionally on Ξ , the locations of satellites on each orbit $l(\rho_i, \theta_i, \phi_i)$ are modeled as a homogeneous Poisson point process ψ_i of intensity $\mu/(2\pi\rho_i)$ on this orbit. Equivalently, the orbital angles of satellites on each orbit are modeled as a 1-dim homogeneous Poisson point process ψ_i on segment $[0, 2\pi)$ of intensity $\mu/(2\pi)$. Since the satellites are distributed conditionally on Ξ , the satellite point process Ψ is a Cox point process. The satellite Cox point process is

$$\Psi = \sum_i \psi_i. \quad (2)$$

Figs. 1 – 2 depict the proposed satellite Cox point process with λ , μ , r_a and r_b . In the figures, we use $\nu(d\rho) = \frac{d\rho}{r_b - r_a}$, i.e., the radii of orbits are uniformly distributed on the interval $[r_a, r_b]$. The proposed model can be used to represent e.g., multiple operators of LEO satellite networks where orbits are at different altitudes. The case of all satellites are located at the same altitude in [10] is a special case of the proposed model by taking $\nu(d\rho) = \delta_{r_a}(d\rho)$, where r_a is the radius of orbits.

B. User Distribution

Users are located on the surface of Earth $\{(x, y, z) | x^2 + y^2 + z^2 = r_e^2\}$ and the locations of network users are assumed to be independent of the locations of the LEO satellites.

Remark 1. *This study aims to understand performance-related essential statistics of the LEO satellite networks with multiple constellations characterized by various multiple geometric parameters including their altitudes. In practice, a given constellation plan includes the number of orbital planes, the inclinations of orbits, their altitudes, and the number of*

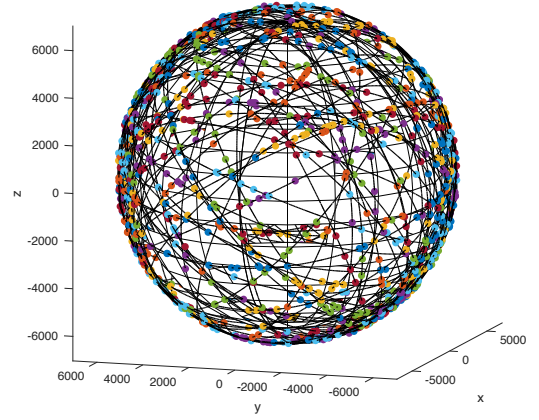


Fig. 1. The proposed Cox satellite model with $r_a = 7000$ km, $r_b = 7050$ km. We use $\lambda = 72$, $\mu = 22$, and $\nu(d\rho) = d\rho/(r_b - r_a)$.

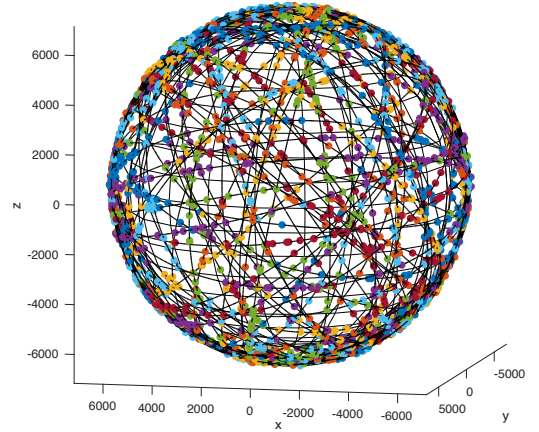


Fig. 2. The Cox-modeled satellite with $r_a = 7000$ km and $r_b = 7500$ km. We use $\lambda = 30$, $\mu = 60$, and $\nu(d\rho) = d\rho/(r_b - r_a)$.

satellites per plane. However, the actual geometry of each LEO satellite constellation may deviate significantly due to practical reasons like satellite retirement, new or delayed satellite launches, and satellite decay. In addition, the reduction in launch costs has facilitated the emergence of numerous LEO satellite constellations, and this trend is expected to continue, making the scenario of the collection of constellations increasingly complex. As a result, obtaining precise information about all satellites' locations and inclinations becomes highly challenging. This justifies considering the random modeling approach considered not only in this paper but also in previous existing stochastic geometry studies [6]–[9].

III. RESULTS

A. Statistical Results

In this section, we derive/prove (i) the mean number of LEO satellites, (ii) the isotropy of Ψ , (iii) the distances from the LEO satellites to an arbitrarily located user, (iv) the distribution of the distance to the nearest visible satellite, (v) the outage probability, (vi) the Laplace functional of Ψ , and (vii) the Laplace transform of the total interference under general fading. These statistical properties directly determine

the performance of downlink LEO satellite communications in this context.

Lemma 1. *The average number of the proposed Cox satellite point process is $\lambda\mu$.*

Proof: Let \mathcal{S} be the set of all spheres with radii from r_a to r_b . The average number of satellites is given by

$$\begin{aligned} \mathbf{E}[\Psi(\mathcal{S})] &= \mathbf{E}\left[\sum_{Z_i \in \Xi} \mathbf{E}\left[\sum_{X_j \in \psi_i} 1 \middle| \Xi\right]\right] \\ &= \mathbf{E}\left[\sum_{Z_i \in \Xi} \int_0^{2\pi} \frac{\mu}{2\pi} dx \middle| \Xi\right] \\ &= \mu \int_0^\pi \int_0^\pi \int_{r_a}^{r_b} \frac{\lambda \sin(\phi)}{2\pi} \nu(d\rho) d\theta d\phi = \lambda\mu, \end{aligned}$$

where we use Campbell's mean value theorem [11]. ■

Below we show that \mathcal{O} is invariant w.r.t. rotations. This allows one to evaluate the performance of network seen by a typical user at the north pole.

Lemma 2. *The distribution of \mathcal{O} and Ψ are isotropic.*

Proof: Let \mathbb{S} be the unit sphere of center O . Let U be a uniformly distributed random point on \mathbb{S} . For each U , there is a unique directed orbit $\mathbb{O}(U) \subset \mathbb{S}$ the orbit whose right-hand rule normal vector is \overline{OU} . Note that $\mathbb{O}(U)$ is a factor of U ; namely, for all \mathbb{R}^3 rotations R of center o , the orbit $\mathbb{O}(R(U))$ coincides with the orbit $R(\mathbb{O}(U))$. Since the law of U is isotropic on \mathbb{S} , it follows from the relation $\mathbb{O}(R(U)) = R(\mathbb{O}(U))$ that the law of $\mathbb{O}(U)$ is also isotropic.

It is well known that the uniform vector U can be represented as $U = (\sqrt{1-V^2} \cos(\Theta), \sqrt{1-V^2} \sin(\Theta), V)$ with $V \sim \text{Uniform}(-1, 1)$, $\theta \sim \text{Uniform}(0, 2\pi)$, and $V \perp \Theta$.

For the directed orbit $\mathbb{O}(U)$, let $\theta \in [0, 2\pi)$ to be the angle of the ascending point from the x -axis and $\phi \in [0, \pi)$ to be the azimuth of the normal vector. Then, ϕ coincides with the inclination in this paper. Using the distributions of V and Θ , we get

$$\phi = \arccos(V) \quad \text{and} \quad \theta = \Theta + \pi/2 \pmod{2\pi}. \quad (3)$$

Since $V \perp \Theta$, we get $\phi \perp \theta$. Using Eq. (3), we have $\theta \sim \text{Uniform}[0, 2\pi)$ and the PDF of ϕ as follows:

$$f_\phi(x) = \frac{\sin(x)}{2} \text{ for } 0 \leq x < \pi \text{ and } 0 \text{ otherwise.} \quad (4)$$

The isotropic directed orbit Poisson point process can hence be represented as a Poisson point process of density $\Lambda(\theta, \phi) = \frac{\lambda}{4\pi} \sin(\phi)$ on the rectangle set $\mathcal{R} = [0, \pi) \times [0, 2\pi)$. Here, λ is the mean number of directed orbits.

Furthermore, the directed orbit with angles (θ, ϕ) and the directed orbit with angles $(\theta + \pi, \phi + \pi/2 \pmod{\pi})$ reduce to the same orbit when forgetting the orbit direction. Therefore, for the undirected isotropic orbit, its longitude angle $\tilde{\theta}$ is uniformly distributed in $[0, \pi)$. The isotropic undirected orbit Poisson point process can hence be represented as a Poisson point process of density $\tilde{\Lambda}(\tilde{\phi}, \tilde{\theta}) = \frac{\lambda}{2\pi} \sin(\tilde{\phi})$ on the rectangle set $\tilde{\mathcal{R}} = [0, \pi) \times [0, \pi)$.

Finally, since the proposed orbit process density is defined as the product form $\frac{\lambda \sin(\phi)}{2\pi} \nu(d\rho)$, \mathcal{O} is isotropic and hence Ψ is isotropic. ■

Lemma 3. *Consider a satellite X of orbital angle ω_j on the orbit $l(\rho_i, \theta_i, \phi_i)$. The distance from $(0, 0, r_e)$ to the satellite $X(\rho_i, \theta_i, \phi_i, \omega_j)$ is given by*

$$\sqrt{\rho_i^2 - 2\rho_i r_e \sin(\omega_j) \sin(\phi_i) + r_e^2}. \quad (5)$$

Proof: The coordinates $(x, y, z) \in \mathbb{R}^3$ of the satellite that has the orbital angle ω_j on the orbit $l(\rho_i, \theta_i, \phi_i)$ are given by

$$x = \sqrt{\rho_i^2 \cos^2(\omega_j) + \rho_i^2 \sin^2(\omega_j) \cos^2(\phi_i)} \cos(\tilde{\theta} + \theta_i), \quad (6)$$

$$y = \sqrt{\rho_i^2 \cos^2(\omega_j) + \rho_i^2 \sin^2(\omega_j) \cos^2(\phi_i)} \sin(\tilde{\theta} + \theta_i), \quad (7)$$

$$z = \rho_i \sin(\omega_j) \sin(\phi_i), \quad (8)$$

$$\tilde{\theta} = \arctan(\tan(\omega_j) \cos(\phi_i)), \quad (9)$$

where ϕ is the inclination of the orbit.

As a result, the distance from $(0, 0, r_e)$ to the satellite is

$$\|(x, y, z) - (0, 0, r_e)\| = \sqrt{\rho_i^2 - 2\rho_i r_e \sin(\omega_j) \sin(\phi_i) + r_e^2}.$$

Note the distance is independent of the variable θ . ■

Since (i) users are independent of Ψ and (ii) Ψ is invariant by rotations (Lemma 2), one can consider a typical user at $(0, 0, r_e)$ and study the network performance it experiences, which will be typical.

Let $C(d)$ be the subset of \mathcal{S} such that the distances from the typical observer u to the satellites on $C(d)$ are less than a distance d . For any $r_a \leq \rho \leq r_b$, we define

$$\begin{aligned} C(d) &= \bigcup_{r_a \leq \rho \leq r_b} C(\rho, d) \\ &= \bigcup_{r_a \leq \rho \leq r_b} \{(x, y, z) \in \mathbb{R}^3 \mid z \geq r_e, x^2 + y^2 + z^2 = \rho^2, \\ &\quad x^2 + y^2 + (z - r_e)^2 \leq d^2\}, \end{aligned}$$

where $z \geq r_e$, since satellites with z -coordinates less than r_e are invisible to the user at $(0, 0, r_e)$. $C(\rho, d)$ is a spherical cap associated with the orbit of radius ρ . See Fig. 3.

Lemma 4. *The length of the arc given by the intersection of the spherical cap $C(\rho, d)$ and the orbit $l(\rho, \theta, \phi)$ is*

$$2\rho \arcsin\left(\sqrt{1 - \left(\frac{\rho^2 + r_e^2 - d^2}{2\rho r_e \sin(\phi)}\right)^2}\right), \quad (10)$$

for $\rho - r_e \leq d \leq \sqrt{\rho^2 - r_e^2}$.

Proof: Consider $C(\rho, d)$. Let ξ be the angle $\angle AOU$ in Fig. 3. Then, we use the law of Cosine to obtain $\cos(\xi) = (\rho^2 + r_e^2 - d^2)/(2\rho r_e)$.

For the triangle $\triangle BCD$, we have $\overline{CD} = \rho \cos(\xi) \cot(\phi)$. Since the angle $\angle BDC$ is $\pi/2$, we obtain

$$\overline{BD} = \sqrt{\rho^2 \sin^2(\xi) - \rho^2 \cos^2(\xi) \cot^2(\phi)}.$$

For $\triangle BOD$, $\overline{OB} = \rho$ and let $\kappa' = \angle BOD$. Then we have

$$\sin(\kappa') = \overline{BD}/\rho = \sqrt{\sin^2(\xi) - \cos^2(\xi) \cot^2(\phi)}.$$

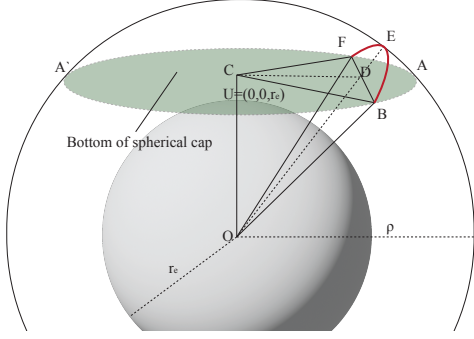


Fig. 3. The arc of orbit $l(\rho, \theta, \phi)$ in spherical cap $C(\rho, d)$.

Finally, the length of the arc \widehat{BF} is given by

$$\nu(\widehat{BF}) = 2\rho \arcsin(\sqrt{1 - \cos^2(\xi) \csc^2(\phi)}).$$

where $\cos(\xi) = (\rho^2 + r_e^2 - d^2)/(2\rho r_e)$. ■

In downlink LEO satellite communication networks, network users are meant to receive signals from their closest or nearest satellites [9]. The distance D from a network user to its closest LEO satellite is a random variable. When there is no visible satellite, $D \stackrel{def}{=} \infty$.

Lemma 5. *The cumulative distribution function of D is given by Eq. (11) where $\cos(\xi) = (\rho^2 + r_e^2 - d^2)/(2\rho r_e)$.*

Proof: For $r_a - r_e \leq d \leq \sqrt{r_b^2 - r_e^2}$, we have

$$\begin{aligned} \mathbf{P}(D > d) &\stackrel{(a)}{=} \mathbf{P}(\|X - u\| > d, \forall X \in \Psi) \\ &\stackrel{(b)}{=} \mathbf{P}(\|X_j - u\| > d, \forall X_j \in \psi_i, \forall Z_i \in \Xi) \\ &= \mathbf{P}\left(\prod_{Z_i \in \Xi} \mathbf{P}\left(\prod_{X_j \in \psi_i} \|X_j - u\| > d \mid \Xi\right)\right). \end{aligned}$$

To get (a), we use the fact that for $R > r$, all satellites should be at distances greater than r . We have (b) by using that the Cox satellite point process is comprised of the Poisson point processes conditionally on orbits. We have

$$\begin{aligned} &\mathbf{P}\left(\prod_{X_j \in \psi_i} \|X_j - u\| > r \mid \Xi\right) \\ &= \exp\left(-\mu\pi^{-1} \arcsin\left(\sqrt{1 - \cos^2(\xi) \csc^2(\phi_i)}\right)\right), \end{aligned}$$

where $\cos(\xi) = (\rho_i^2 + r_e^2 - d^2)/(2\rho_i r_e)$, as a function of the orbits' radius. We use the facts that (i) in order to have no point at distance less than r , the arc created by the orbit $l(\rho_i, \phi_i, \theta_i)$ and the set $C(\rho_i, d)$ has to be empty of satellite points and (ii) the void probability of the Poisson point process of intensity μ on the arc is given by the negative exponential of μ times the arc length. Leveraging the facts that only the orbits with

inclinations $\pi/2 - \xi < \phi < \pi/2 + \xi$ meet the spherical cap $C(d)$, we have

$$\begin{aligned} &\mathbf{P}(D > d) \\ &= \mathbf{P}\left(\prod_{Z_i \in \Xi} e^{-\mu\pi^{-1} \arcsin\left(\sqrt{1 - \cos^2(\xi) \csc^2(\phi_i)}\right)}\right) \\ &= \exp\left(-\lambda \int_{r_a}^{r_b} \int_0^\xi \left(1 - e^{-\frac{\mu}{\pi} \arcsin\left(\sqrt{1 - \frac{\cos^2(\xi)}{\cos^2(\varphi)}}\right)}\right) \cos(\varphi) d\varphi \nu(d\rho)\right), \end{aligned}$$

where we use the change of variable $\phi = \pi/2 - \varphi$, $\cos(\xi) = (\rho^2 + r_e^2 - d^2)/(2\rho r_e)$, and the probability generating functional of the Poisson point process Ξ . ■

Definition 1. *Outage occurs if the typical network user has no visible satellite. Equivalently, outage occurs if $D = \infty$.*

Lemma 6. *The outage probability is given by Eq. (12).*

Proof: When there is no visible satellite, $D = \infty$. By using Lemma 5, the outage probability is given by

$$\begin{aligned} &\mathbf{P}(D = \infty) \\ &= \mathbf{P}(\|X_j - u\| > \sqrt{\rho_i^2 - r_e^2}, \forall X_j \in \psi_i, \forall Z_i \in \Xi) \\ &= \mathbf{P}\left(\prod_{Z_i \in \Xi} \mathbf{P}\left(\prod_{X_j \in \psi_i} \|X_j - u\| > \sqrt{\rho_i^2 - r_e^2} \mid \Xi\right)\right), \end{aligned}$$

where we have

$$\begin{aligned} &\mathbf{P}\left(\prod_{X_j \in \psi_i} \|X_j - u\| > \sqrt{\rho_i^2 - r_e^2} \mid \Xi\right) \\ &= \exp\left(-\mu\pi^{-1} \arcsin\left(\sqrt{1 - r_e^2 \csc^2(\phi_i)/\rho_i^2}\right)\right). \end{aligned}$$

We use the fact that when $d = \sqrt{\rho_i^2 - r_e^2}$, $\cos(\xi) = r_e/\rho_i$. In other words, for a given ρ , the orbits with inclinations $\pi/2 - \xi < \phi < \pi/2 + \xi$ meet the spherical cap $C(\rho, \sqrt{\rho^2 - r_e^2})$.

The outage probability is then given by

$$\begin{aligned} &\mathbf{P}\left(\prod_{Z_i \in \Xi} e^{-\mu\pi^{-1} \arcsin\left(\sqrt{1 - r_e^2 \csc^2(\phi_i)/\rho_i^2}\right)}\right) \\ &= \exp\left(-\lambda \int_{r_a}^{r_b} \int_0^{\arccos(r_e/\rho)} \left(1 - e^{-\frac{\mu}{\pi} \arcsin\left(\sqrt{1 - r_e^2 \sec^2(\varphi)/\rho^2}\right)}\right) \cos(\varphi) d\varphi \nu(d\rho)\right), \end{aligned}$$

where we use the change of variable $\phi = \pi/2 - \varphi$ and then the probability generating functional of Ξ . ■

Fig. 4 shows the outage probability obtained by Lemma 6.

Lemma 7. *Consider a function $f(X) : \mathbb{R}^3 \rightarrow \mathbb{R}$. The Laplace functional of the Cox point process is defined by $\mathcal{L}_\Psi(f) = \mathbf{E}_\Psi[\exp(-\sum_{X_i \in \Psi} f(X_i))]$. The Laplace functional is given by Eq. (13) where $\mathcal{C} = [r_a, r_b] \times [0, \pi) \times [0, \pi)$.*

$$\mathbf{P}(D > d) = \exp \left(-\lambda \int_{r_a}^{r_b} \int_0^\xi \left(1 - e^{-\mu \pi^{-1} \arcsin(\sqrt{1 - \cos^2(\xi) \sec^2(\varphi)})} \right) \cos(\varphi) d\varphi \nu(d\rho) \right), \quad (11)$$

$$\mathbf{P}(D = \infty) = \exp \left(-\lambda \int_{r_a}^{r_b} \int_0^{\arccos(r_e/\rho)} \left(1 - e^{-\mu \pi^{-1} \arcsin(\sqrt{1 - r_e^2 \sec^2(\varphi)/\rho^2})} \right) \cos(\varphi) d\varphi \nu(d\rho) \right), \quad (12)$$

$$\mathcal{L}(f) = \exp \left(-\frac{\lambda}{2\pi} \int_{r_a}^{r_b} \int_0^\pi \int_0^\pi \left(1 - e^{-\frac{\mu}{2\pi} \int_0^{2\pi} 1 - \exp(-\bar{f}(\rho, \theta, \phi, \omega)) d\omega} \right) \sin(\phi) d\phi d\theta \nu(d\rho) \right), \quad (13)$$

$$\mathcal{L}_\Psi(f)_{f=sH\|X-U\|^{-\alpha}} = \exp \left(-\frac{\lambda}{2\pi} \int_{\bar{\mathcal{C}}} \left(1 - e^{-\frac{\mu}{2\pi} \int_{\bar{\omega}} 1 - \mathcal{L}_H(s(\rho^2 - 2\rho r_e \sin(\omega) \sin(\phi) + r_e^2)^{-\frac{\alpha}{2}}) d\omega} \right) \sin(\phi) d\phi d\theta \nu(d\rho) \right). \quad (14)$$

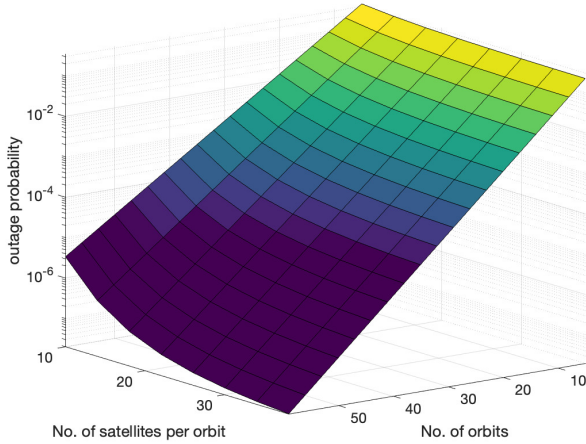


Fig. 4. The outage probability with $r_a = 7000$ km and $r_b = 7500$ km. We use $\lambda = 72$, $\mu = 22$, and $\nu(d\rho) = d\rho/(r_b - r_a)$.

Proof: The Laplace functional of the satellite Cox point process is given by

$$\begin{aligned} \mathcal{L}_\Psi(f) &= \mathbf{E} \left[e^{-\sum_{X \in \Psi} f(X)} \right] \\ &= \mathbf{E}_\Xi \left[\mathbf{E}_\psi \left[e^{-\sum_{Z_i \in \Xi} \sum_{X_j \in \psi_i} f(X)} \middle| \Xi \right] \right] \\ &= \mathbf{E}_\Xi \left[\prod_{Z_i \in \Xi} \exp \left(-\frac{\mu}{2\pi} \int_0^{2\pi} 1 - e^{-\bar{f}(\rho_i, \theta_i, \phi_i, \omega)} d\omega \right) \right] \\ &= \exp \left(-\frac{\lambda}{2\pi} \int_{r_a}^{r_b} \int_0^\pi \int_0^\pi \left(1 - e^{-\frac{\mu}{2\pi} \int_0^{2\pi} 1 - \exp(-\bar{f}(\rho, \theta, \phi, \omega)) d\omega} \right) \sin(\phi) d\phi d\theta \nu(d\rho) \right), \end{aligned}$$

where we use the function $\bar{f}(\rho, \theta, \phi, \omega) = f(X)$ for any satellite X on the orbit $l(\rho, \theta, \phi)$ with its orbital angle ω . Then, we use the probability generating functional of the Poisson point process Ξ to get the final result. ■

Consider a random variable H modeling general fading. A received signal power of a user at u is then given by $f(X) = H\|X - u\|^{-\alpha}$ where X is the location of the satellite and α is the path loss exponent. The total interference S is then given

by the sum of the received signal powers from all satellites.

$$S = \sum_{X \in \bar{\Psi}} H\|X - u\|^{-\alpha}, \quad \bar{\Psi} = \Psi \left(\bigcup_{r_a < \rho \leq r_b} C(\rho, \sqrt{\rho^2 - r_e^2}) \right).$$

Corollary 1. The Laplace transform of the total interference is given by Eq. (14) where $\bar{\mathcal{C}} = \{(\rho, \theta, \phi) \in l(\rho, \theta, \phi) \cap C(\sqrt{r_b^2 - r_a^2}) \neq \emptyset\}$ and $\bar{\omega} = \{\omega \in [0, 2\pi] | X(\rho, \theta, \phi, \omega) \in C(\sqrt{r_b^2 - r_a^2}), \forall (\rho, \theta, \phi) \in \bar{\mathcal{C}}\}$.

Proof: The Laplace transform in question is

$$\begin{aligned} \mathcal{L}_\Psi(f)_{f=sH\|X-U\|^{-\alpha}} &= \mathbf{E}_\Xi \left[\mathbf{E}_\psi \left[e^{-\sum_{Z_i \in \Xi} \sum_{X_j \in \psi_i} sH\|X_j - u\|^{-\alpha}} \middle| \Xi \right] \right] \\ &= \mathbf{E}_\Xi \left[\prod_{Z_i \in \Xi} \mathbf{E}_\psi \left[\prod_{X_j \in \psi_i} \mathcal{L}_H(s\|X_j - u\|^{-\alpha}) \right] \right], \end{aligned}$$

where $\mathcal{L}_H(\kappa)$ is the Laplace transform of the random variable H . Using a technique similar to Lemmas 3 and 7, we obtain the final result. ■

B. Example: Numerical Comparison

The primary objective of this paper is to introduce an analytical framework that offers a mathematical representation of both existing and future LEO satellite networks. These networks encompass multiple distinct LEO satellite constellations, each characterized by unique network parameters. In this section, we illustrate the application of our proposed Cox satellite model by comparing it to a prospective LEO satellite constellation. Specifically, we conduct a comparison based on the coverage probability of the users in those two different scenarios. To facilitate this comparison, we assume that users are located at a latitude of 30 degrees.

For the future LEO constellation, we employ the Starlink 2A plan [12] and detailed in Table I. Conversely, for our proposed Cox model, we adjust the local density parameters λ and μ to ensure the average numbers of LEO satellites are the same across all two scenarios. We assume a Nakagami m fading with path loss exponent 2. Figure 5 depicts the SINR coverage probability for users at a latitude of 30 degrees, considering a frequency reuse factor of 30.

The graph clearly illustrates that our proposed Cox model closely approximates the actual coverage probability of the forthcoming Starlink 2A constellation [12]. This highlights the

TABLE I
STARLINK PHASE 1 SECOND GENERATION

Group	Altitude	Incl.	Count	Sat.	Total
2A – 5	530 km	43°	28	120	3360
2A – 6	525 km	53°	28	120	3360
2A – 7	535 km	33°	28	120	3360

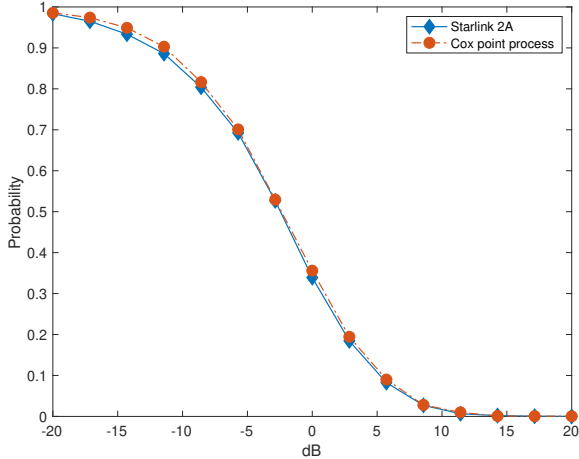


Fig. 5. The SINR coverage probability of the typical user at latitude 30°. For a small scale fading, we use Nakagami- m fading with $m = 1$.

potential of our analytical model in effectively approximating the behavior of future LEO satellite constellations.

It is important to emphasize that unlike the binomial point process model in [6]–[9], our proposed Cox model captures the essential geometric fact that in any LEO satellite constellations, satellites are exclusively on orbits and the satellites’ motions are confined to the orbits. Consequently, our proposed model not only facilitates the analysis of stationary characteristics of the LEO satellite networks, such as shown for the coverage probability but also enables us to explore the dynamic behaviors of LEO satellite networks such as typical delays and delay distributions.

Remark 2. *To get the same local numbers of LEO satellites between the Starlink and Cox constellations, we vary λ , μ , or both of the Cox model. In other words, there exist numerous ways to represent a given LEO satellite constellation. A more comprehensive exploration of how to manage and set these geometric variables is left for future research.*

IV. CONCLUSION

This paper builds a novel stochastic geometry framework for modeling the spatial distribution of clustered LEO satellites along orbits of varying altitudes, achieved through the development of an isotropic Cox point process. The paper explicitly provides expressions for essential statistical properties, including the distribution of nearest distances to LEO satellites, outage probability, the Laplace function of the Cox point process, and the Laplace transform of the total interference experienced by a typical user. These outcomes can be directly

employed to assess the typical performance of multi-altitude LEO satellite downlink communications.

To showcase the effectiveness of the proposed model, we compare it with a future LEO satellite constellation and a binomial point process. This comparison demonstrates that the proposed model accurately represents forthcoming LEO constellations and can serve as a suitable alternative to existing binomial point process models for LEO satellites, especially considering that LEO satellites in practice are clustered along orbits.

Future work will encompass: (i) analyzing the coverage probability of the typical user, (ii) evaluating the satellite coverage area beneath the Cox-modeled satellites, and (iii) extending the framework to include a fixed-inclination orbit process.

ACKNOWLEDGMENT

The work of Chang-Sik Choi was supported by the NRF-2021R1F1A1059666. The work of François Baccelli was supported by the ERC NEMO grant 788851 to INRIA.

REFERENCES

- [1] Y. Su, Y. Liu, Y. Zhou, J. Yuan, H. Cao, and J. Shi, “Broadband LEO satellite communications: Architectures and key technologies,” *IEEE Wireless Commun.*, vol. 26, no. 2, pp. 55–61, 2019.
- [2] Z. Qu, G. Zhang, H. Cao, and J. Xie, “LEO satellite constellation for Internet of Things,” *IEEE Access*, vol. 5, pp. 18 391–18 401, 2017.
- [3] J. Khalife, M. Neinavaie, and Z. M. Kassas, “The first carrier phase tracking and positioning results with starlink LEO satellite signals,” *IEEE Trans. Aerospace and Electronic Syst.*, vol. 58, no. 2, pp. 1487–1491, 2022.
- [4] A. Guidotti, A. Vanelli-Coralli, M. Conti, S. Andrenacci, S. Chatzinotas, N. Maturo, B. Evans, A. Awoseyila, A. Ugolini, T. Foggi, L. Gaudio, N. Alagha, and S. Cioni, “Architectures and key technical challenges for 5G systems incorporating satellites,” *IEEE Trans. Veh. Technol.*, vol. 68, no. 3, pp. 2624–2639, 2019.
- [5] 3GPP TR 38.821, “Solutions for NR to support non-terrestrial networks (NTN),” *3GPP TR 38.821*.
- [6] N. Okati, T. Riihonen, D. Korpi, I. Angervuori, and R. Wichman, “Downlink coverage and rate analysis of low earth orbit satellite constellations using stochastic geometry,” *IEEE Trans. Commun.*, vol. 68, no. 8, pp. 5120–5134, 2020.
- [7] A. Talgat, M. A. Kishk, and M.-S. Alouini, “Stochastic geometry-based analysis of LEO satellite communication systems,” *IEEE Commun. Lett.*, vol. 25, no. 8, pp. 2458–2462, 2021.
- [8] D.-H. Na, K.-H. Park, Y.-C. Ko, and M.-S. Alouini, “Performance analysis of satellite communication systems with randomly located ground users,” *IEEE Trans. Wireless Commun.*, vol. 21, no. 1, pp. 621–634, 2022.
- [9] D.-H. Jung, J.-G. Ryu, W.-J. Byun, and J. Choi, “Performance analysis of satellite communication system under the shadowed-rician fading: A stochastic geometry approach,” *IEEE Trans. Commun.*, vol. 70, no. 4, pp. 2707–2721, 2022.
- [10] C.-S. Choi and F. Baccelli, “An analytical framework for downlink LEO satellite communications based on Cox point processes,” *arXiv preprint arXiv:2212.03549*, 2022.
- [11] F. Baccelli and B. Błaszczyszyn, “Stochastic geometry and wireless networks: volume I theory,” *Foundations and Trends in Networking*, vol. 3, no. 3–4, pp. 249–449, 2010.
- [12] Space exploration holdings, LLC, request for orbital deployment and operating authority for the SpaceX Gen2 NGSO satellite system. [Online]. Available: <https://docs.fcc.gov/public/attachments/FCC-22-91A1.pdf>